

NUMERICAL SIMULATION OF CONCRETE LABORATORY TEST UNDER IMPACT LOADS

Robert Adamczyk

Department of Civil Engineering
Technical University of Koszalin, Koszalin, Poland
e-mail: adamczyk@tu.koszalin.pl

Tomasz Łodygowski

Institute of Structural Engineering,
Poznań University of Technology, Poznań, Poland
e-mail: Tomasz.Lodygowski@put.poznan.pl

Key words: Computational Mechanics, Dynamics, FEM, Numerical simulations

Abstract. *The aim of this presentation is to reproduce in computations the experimental results of behaviour of concrete cylinder specimen loaded by compression impact, studied by P.H. Bischoff and S.H. Perry [2]. The reported investigation is also focused on creation of constitutive relation for concrete dependent on strain velocities. The accuracy of the numerical results was studied and compared with the experiment. The new model, calibrated for this simple laboratory test, was used in numerical simulations of more complicated impact loaded concrete elements. The analysis was carried out in the environment of ABAQUS finite element code [1].*

1. Introduction

In practice, engineers often meet the problem how to estimate the behaviour of structures in case of high strain rates. Usually, the problems seem to be far complex, because there is no possibility of carry out any experimental searches in real scale due to economic reasons or difficulties in measuring required values. In these cases the engineering design could be strongly supported by computer simulations.

Among other problems to be solved, like building discrete model of such simulation, the fundamental importance has been focused on constitutive modelling.

Due to highly nonlinear, rate-dependent behaviour of plain concrete, adoption of any model in the analysis is relatively complex and its application into finite element computer code is difficult. Some comments and considerations concerning various aspects of numerical simulations of such phenomena were presented by Cichocki *et al.* [3].

To investigate complex engineering concrete structures under impact loading it is necessary to formulate proper constitutive model of the material. Quantitatively, it is easy to observe, in known laboratory experiments, that model should depend on strain rates and include the failure criteria. It seems to be relatively easy to verify constitutive properties using uniaxial tests. This test can also serve to calibrate the constitutive parameters. The numerical simulation strongly supports this process. The procedure we propose for solving complex engineering problems using simple uniaxial laboratory tests is illustrated in box schema in Fig. 1.

The goal of the study is to verify the constitutive properties using uniaxial test (the impact test setup is schematically shown in Fig. 2.) This test can serve for calibration of the constitutive parameters, which then could be later used, in more complex structural, boundary value problems.

Finally, we have proposed new rate dependent, elastic-plastic constitutive model for concrete that include tensile failure criterion. The bases for estimation rate dependent characteristics for concrete, were the static characteristics given in [2] and experimental equations proposed in [4]. The rate dependence was taken into consideration as an increase of strength, elastic modulus and strain in function of strain rate. The proposed numerical model was used to investigate the response of plain concrete cylinder (specimen) under uniaxial compression test reported in [2].

Results for two different concrete classes: 30 MPa and 50 MPa and three different rates of strains: 9 s^{-1} , 5.2 s^{-1} and 5.6 s^{-1} (experiment [2]) were compared. The results for static test were also in focus of interests.

2. Experimental motivation

Specimens were of cylindrical shape with diameter of 101.6 mm and height of 254 mm. Two mixes of concrete were considered: 30 MPa and 50 MPa. Quasi static tests took between 300 and 350 s until maximum strength was reached. The impact load was applied by drop of a mass on the specimen. Specimens were loaded between rigid plates, and a constant rate of

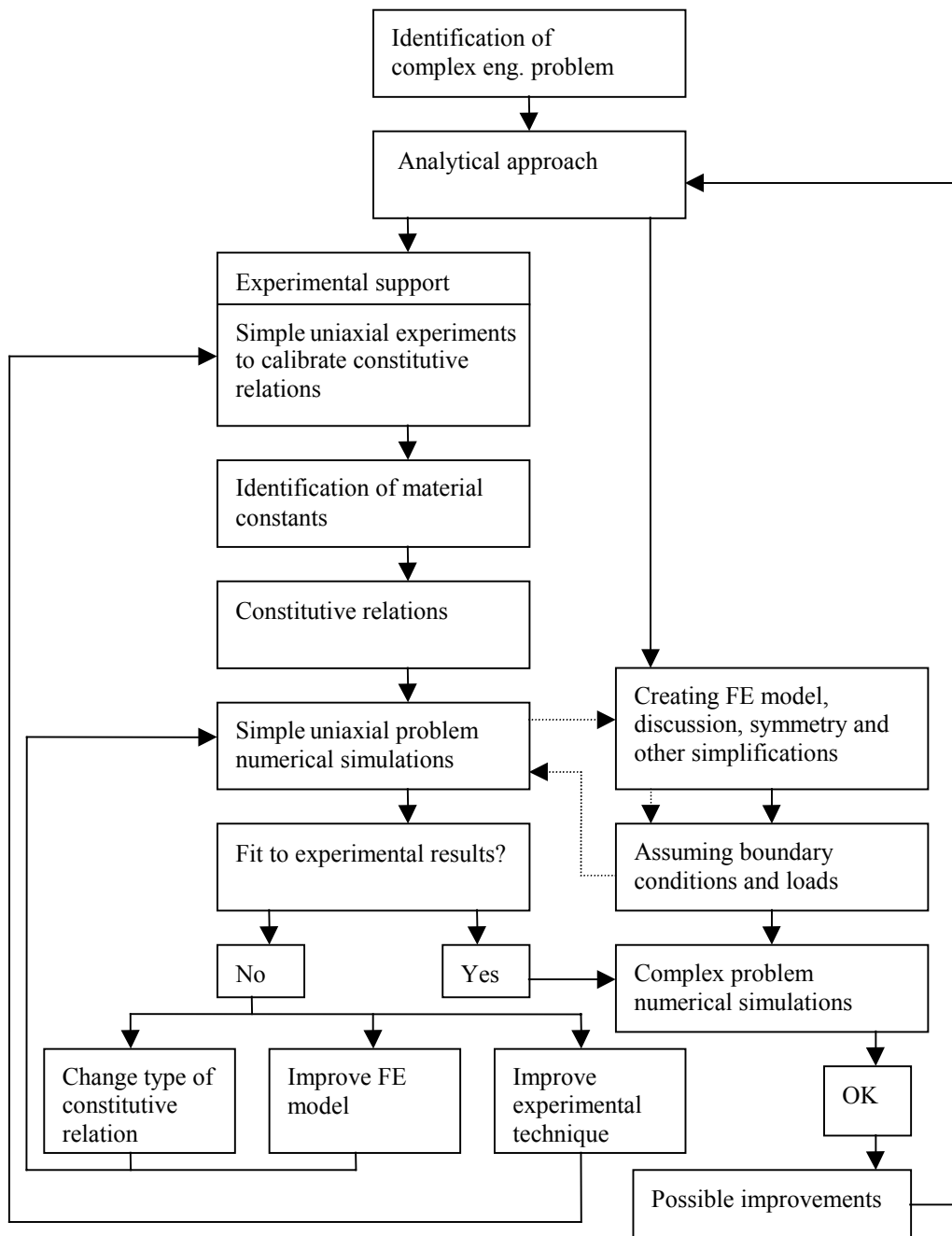


FIG. 1. Interaction between numerical simulation and laboratory tests in searching the constitutive relation

displacement was maintained during testing using an RDP servocontrolled closed-loop loading system to control movement of the loading platen. Deformation was measured with two axial and two circumferential PL-60 strain gauges (60 mm gauge length) placed diametrically opposite one to another, respectively, in the central zone of the cylinder. Load and strain gauge deformation readings were recorded at specific intervals during continuous application of loads. Stress was then calculated by dividing the measured load by the initial cross-section area of specimen. Impact tests were loaded to failure within 300 - 450 μ s with

the drop hammer machine shown schematically in Fig. 2 (for details see [6]). The 31.6 kg mass was used in impact tests at velocities 8 - 8.35 m/s and the 78.3 kg mass was used at velocities of 5 - 5.5 m/s. The deformation of concrete were measured with strain gauges in a manner similar to that described for static tests. Analogue-to-digital transient recorders were used to record load and strain at $5\mu\text{s}$ intervals (200 kHz sampling frequency). Axial compressive stress was measured at the base of the concrete specimens using a thin pressure load cell designed to minimize errors caused by stress - waves reflection within the load cell. The pressure load cell consist of manganin foil pressure gauges was embedded by a very thin layer of epoxy resin and sandwiched between two 5 mm thick aluminium plates.

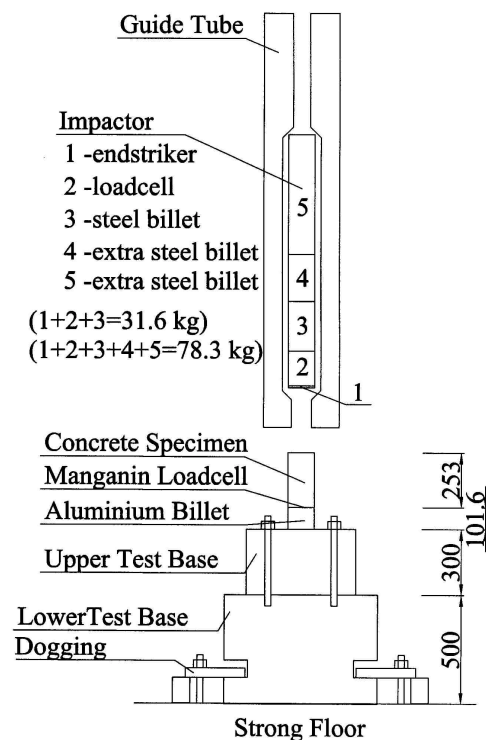


FIG. 2. Schematic view of impact test setup

3. Experimental achievements

In dynamics for the concrete, the increase of dynamic values of elasticity modulus E_b^d due to static elasticity modulus E_b^{st} is observed. Strains corresponding to dynamic strength ϵ_R^d also change due to static strains ϵ_R^{st} . Experimental results show that these values increase if the level of strain rate increases. The changes can be described by experimental equations (3.1) and (3.2), see [5]:

$$(3.1) \quad \frac{E_{bt}^d}{E_{bt}^{st}} = 1.061 + 0.0464 \cdot \log \dot{\varepsilon} + 0.00683 \cdot \left(\log \dot{\varepsilon} \right)^2,$$

$$(3.2) \quad \frac{\varepsilon_R^d}{\varepsilon_R^{st}} = 1.08 + 0.112 \cdot \log \dot{\varepsilon} + 0.0193 \cdot \left(\log \dot{\varepsilon} \right)^2.$$

The factor of dynamic strength increase taken into consideration in this analysis is described by:

$$(3.3) \quad k_d = \frac{R_b^d}{R_b^{st}}.$$

The factor was experimentally appointed [4] and has satisfactory conformity in strain rates:

$$\dot{\varepsilon} = \{1 \cdot 10^{-5} s^{-1} \div 100 s^{-1}\};$$

$$(3.4) \quad k_d \left(\dot{\varepsilon} \right) = 1.53 + 0.21 \cdot \log \dot{\varepsilon} + 0.021 \cdot \left(\log \dot{\varepsilon} \right)^2,$$

where: E_{bt}^d is the initial tangential dynamic elasticity modulus, E_{bt}^{st} is the initial tangential static elasticity modulus, R_b^d and R_b^{st} are the concrete dynamic compressive strength and the concrete static compressive strength, respectively, and ε_R^d is strain corresponding to dynamic compressive strength and ε_R^{st} is strain corresponding to static compressive strength.

4. Numerical model

Impact problem was solved by means of finite element method (FEM) using ABAQUS/Explicit code. Static tests were carried out in the environment of ABAQUS/Standard ver. 5.8.

4.1 Discretisation and boundary conditions

The problem was defined as an axisymmetric, Fig. 3. Four nodes, bilinear axisymmetric, quadrilateral elements with reduced integration and hourglass control (CAX4R), were used to define the geometry of the specimen. The analysis of the influence of the mesh refinement on results was carried out. Five different meshes were considered: mesh 9x20 (180 elements), 9x50 (450 elements), 15x50 (750 elements), 15x100 (1500 elements) and 29x100 (2900 elements). After results comparison, the mesh 15x50 (750 elements) was chosen and used in further analysis. To simplify relation between specimen and base, pure fixing was put in place of whole test base. Additional constraints had to be used on axis of symmetry Z to fulfil axisymmetry conditions.

4.2 Characteristic of impact loading

Concrete specimen was given to dynamic loads by element called „impactor”. Impactor has the same dimensions in all simulations and was defined in the same way as the specimen. The change of its mass was achieved by a change of density. The impact load was defined by initial conditions – velocity acting at all nodes of the impactor. Gravity was also added. Between specimen and impactor contact conditions were assumed. The contact was implemented between slave nodes of specimen and master surface of impactor. Between specimen and impactor a gap of 1 mm was created to observe close up phenomenon. Mass of 31.6 kg was dropped on the specimen of concrete 30 MPa and concrete 50 MPa with average velocities of 8.2 m/s and 5.3 m/s, for which in experiment the impact test rates were estimated as 9.0 s^{-1} and 5.2 s^{-1} . The mass of 87.3 kg was dropped on concrete 50 MPa with the average velocity of 5.3 m/s; for this case the impact test rate was estimated as 5.6 s^{-1} .

In static tests concrete specimens were subjected to loads which generate the stresses approximately equal to compression strength. No impactor was used. The load was defined as a distributed one and directly acted onto specimen. Concretes 30 MPa and 50 MPa were tested under static loads.

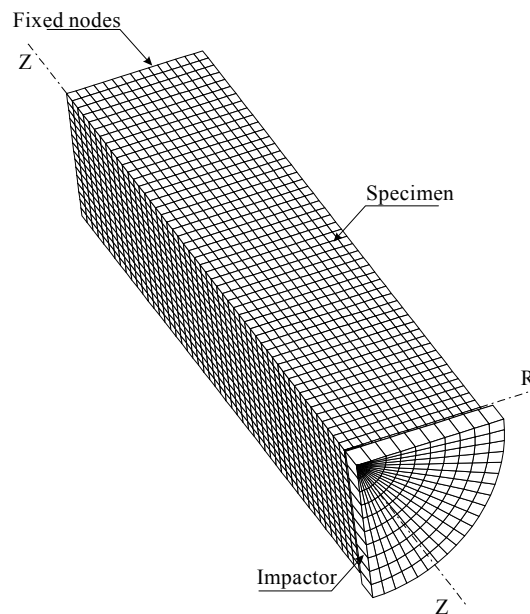


FIG. 3. View of a mesh (axisymmetric angle = 90°) used in computations

4.3 Constitutive assumptions

Constitutive model for concrete taken into impact simulation was elastic – plastic with tensile strength failure criterion. The base for estimating elastic - plastic characteristics was static σ - ε behaviour changed due to experimental equations (3.1 - 3.4). These equations were solved for estimated in tests impact rates. The failure criterion was defined as tensile strength of the concrete in perpendicular direction to compressive load direction. The assumption of this model requires that after meeting failure criterion, deviatoric stress components are set to zero and remain zero for the rest of the calculation, and pressure stress is limited by the hydrostatic cutoff stress [1]. In static simulation no failure criteria was applied.

5. Results of computations

Among others, the values taken in comparisons were $\sigma - \epsilon$ characteristics for impact and static tests. Figs. 3, 4 and 5 show $\sigma - \epsilon$ characteristics for numerical tests compared with lab experiment obtained by Bischoff and Perry [2]. The values were determined as the sum of reaction forces in contact nodes of impactor versus displacement of the contact nodes of the specimen converted due to specimen length.

Compared characteristics $\sigma - \epsilon$ show differences between the results of laboratory tests and numerical simulations. Mostly, this is caused by differences in assumptions that were made. The authors of the tests tried to avoid wave propagation phenomenon in tests using pressure load cell. In numerical simulation we defined no cell, but full fixing of the specimen. The assumption was made because of impossibility of eliminating these effects using any cell. The real value of wave phenomenon in experimental tests then is impossible to estimate. The characteristics $\sigma - \epsilon$ in test are also doubtful, especially the initial parts of them, where there is no any part pointing longitudinal stress wave reflection. In numerical simulation the first peak shows reflecting phenomenon of the longitudinal stress wave (Figs. 4., 5. and 6.), it reflects from the fixed end in a very short time. This peak may be easily estimated in time by the following formula

$$(5.1.) \quad v = \sqrt{\frac{E}{\zeta}},$$

where: v is the wave velocity, E is initial tangent modulus, ζ stays for density. Using the assumption on constant wave velocity and having specimen length, it is easy to estimate time when the wave is reaching the fixed end of the specimen. The height of this peak depends on elastic modulus and density of the material, what we can see in Figs. 4., 5. and 6, and it is independent of value of the striking mass. The curves of lab tests seem to be interpretation of discrete results where wave phenomenon could not be noticed at all, while numerical curves show continuous in time behaviour of the material. In numerical tests the stress was measured as an average reaction force of the impactor on the specimen cross section. In lab tests this was estimated on the base of an average specimen strain. In experiments the rates of deformation are estimated globally (using size of the specimen) at the beginning of the dynamic process, while in computations we discovered the important local differences as an effect of wave propagation and reflection. In spite of these differences, the maximum levels of stresses, in lab tests and numerical simulation after peak part, oscillate around similar values.

The experiments assumed that strain rate was constant and has a certain value for which the test was carried out. It was also assumed that it is constant for the formulation of the problem: (3.1, 3.2, 3.3 and 3.4). However, numerical analysis shows that this rate significantly varies in time.

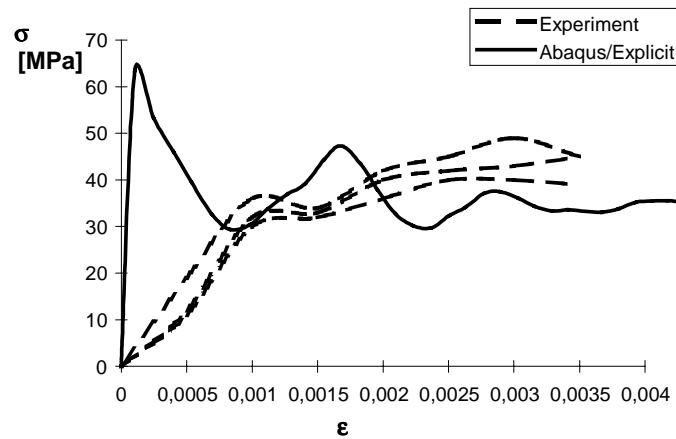


FIG. 4. Characteristics $\sigma - \epsilon$ for concrete 30 MPa, impactor mass = 31.6 kg, initial velocity of impactor $v_0 = 8.2$ m/s, estimated lab test $\dot{\epsilon} = 9$ [1/s]

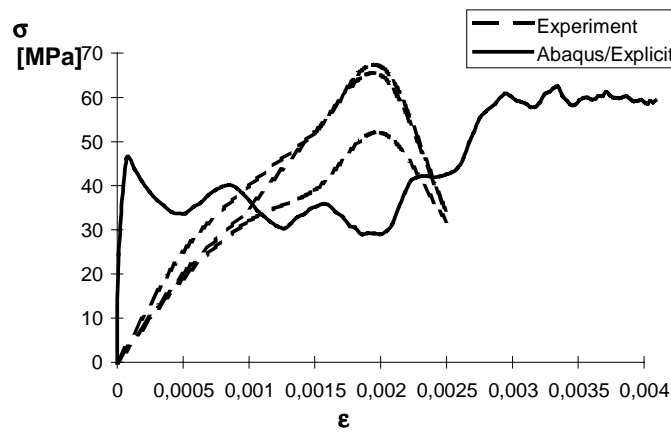


FIG. 5. Characteristics $\sigma - \epsilon$ for concrete 50 MPa, impactor mass = 31.6 kg, initial velocity of impactor $v_0 = 5.3$ m/s estimated lab test $\dot{\epsilon} = 5.2$ [1/s]

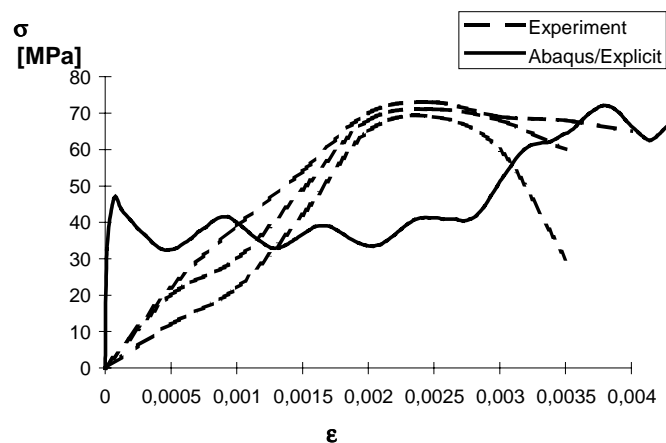


FIG. 6. Characteristics $\sigma - \epsilon$ for concrete 50 MPa, impactor mass = 78.3 kg, initial velocity of impactor $v_0 = 5.3$ m/s, estimated lab test $\dot{\epsilon} = 5.6$ [1/s]

The following figures show the functions of strain rates in the chosen cases versus time.

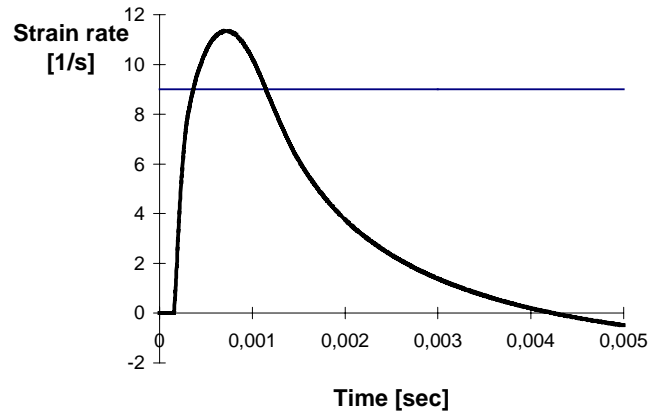


FIG. 7. Strain rate for concrete 30 MPa, impactor mass = 31.6 kg, initial velocity of impactor $v_0 = 8.2$ m/s estimated lab test $\dot{\epsilon} = 9$ [1/s]

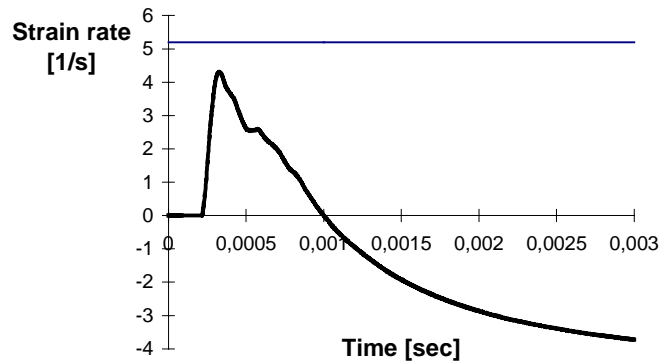


FIG. 8. Strain rate for concrete 50 MPa, impactor mass = 31.6 kg, initial velocity of impactor $v_0 = 5.3$ m/s estimated lab test $\dot{\epsilon} = 5.2$ [1/s]

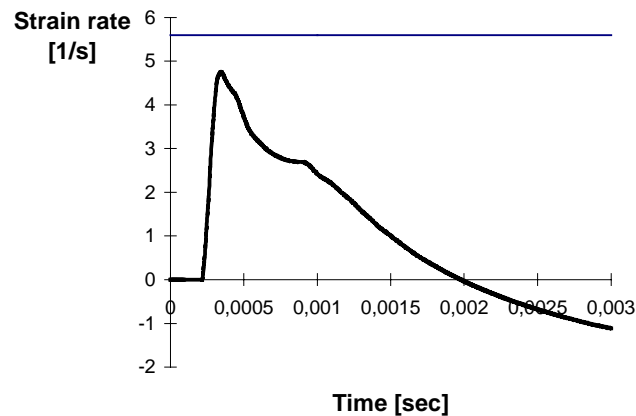


FIG. 9. Strain rate for concrete 50 MPa, impactor mass = 78.3 kg, initial velocity of impactor $v_0 = 5.3$ m/s estimated lab test $\dot{\epsilon} = 5.6$ [1/s]

The maximum values of strain rates differ a bit from the assumed. The accuracy of measuring this value in experimental tests is doubtful. The average strain rate is counted on

the base of measured deformations in time due to strain gauge placed in the middle of the specimen on its surface. In simulation, an average strain is a sum of the nodes displacement in whole cross section in the middle of specimen with respect to specimen height and was considered in time. These rates taken in different cross sections of the specimen exhibit differences, generally the diagram has the same shape but the values are different. This may point out the strongly local phenomenon of strain rate [7].

Reaction force in fixed nodes of the specimen is shown in the following figures (Figs. 10, 11. and 12). It is determined as a sum of reaction force in all fixed nodes of the specimen.

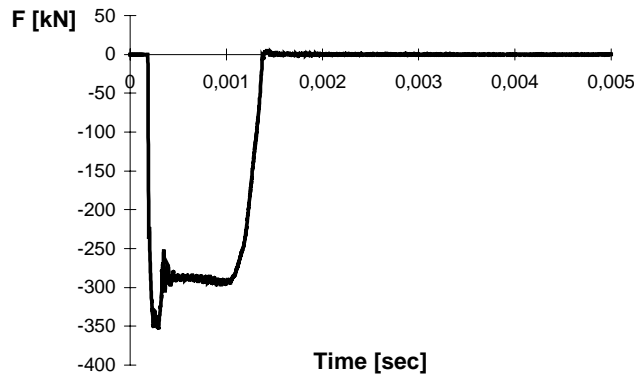


FIG. 10. Reaction force in fixed nodes for concrete 30 MPa, impactor mass = 31.6 kg, initial velocity of impactor $v_0 = 8.2$ m/s

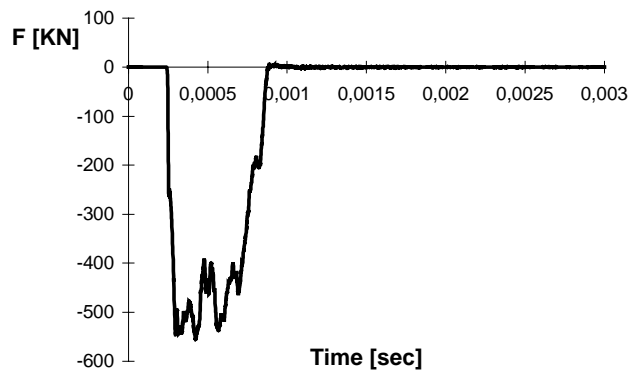


FIG. 11. Reaction force in fixed nodes for concrete 50 MPa, impactor mass = 31.6 kg, initial velocity of impactor $v_0 = 5.3$ m/s

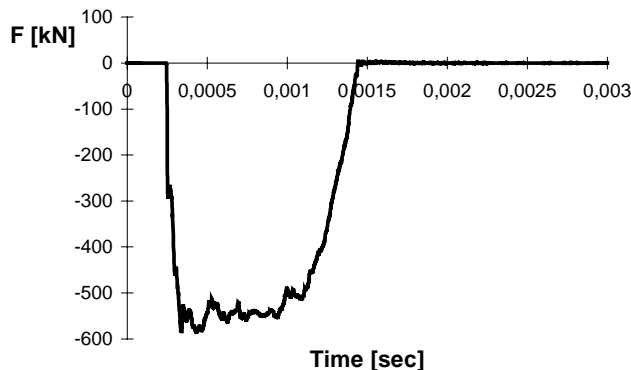


FIG. 12. Reaction force in fixed nodes for concrete 50 MPa, impactor mass = 78.3 kg, initial velocity of impactor $v_0 = 5.3$ m/s

The Figures confirm importance of wave phenomenon in impact compressed specimen. For concrete 30 MPa a peak force reaction is observed after reflection of wave from fix end of the specimen. The time when the reaction force reaches value zero is identified with the moment when the impactor reflects from the specimen.

The following Figures (Figs. 13, 14. and 15) show force versus displacement diagrams for the specimens under consideration. The force is determined as a sum of reaction forces in all nodes of impactor. Displacement is determined as an average displacement of contact nodes of specimen. Wave phenomenon is strongly noticed.

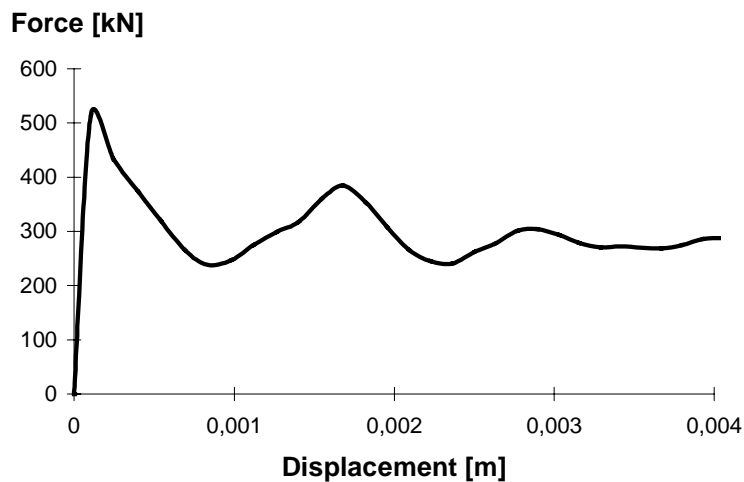


FIG.13. Force versus displacement for concrete 30 MPa, impactor mass = 31.6 kg, initial velocity of impactor $v_0=8.2$ m/s

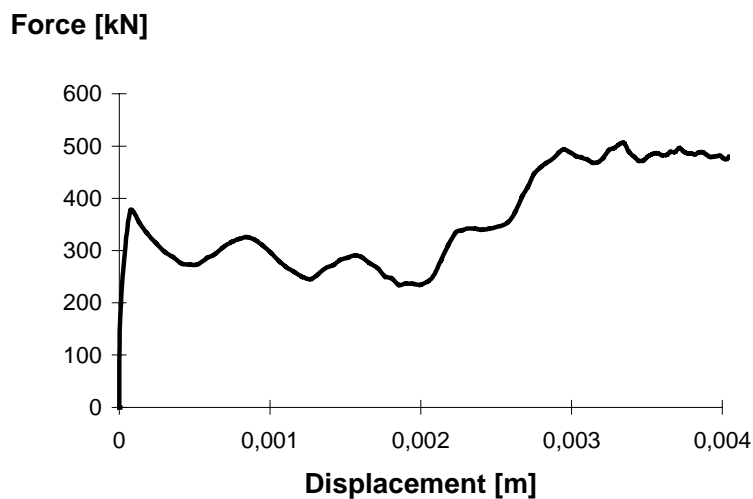


FIG.14. Force versus displacement for concrete 50 MPa, impactor mass = 31.6 kg, initial velocity of impactor $v_0=5.3$ m/s

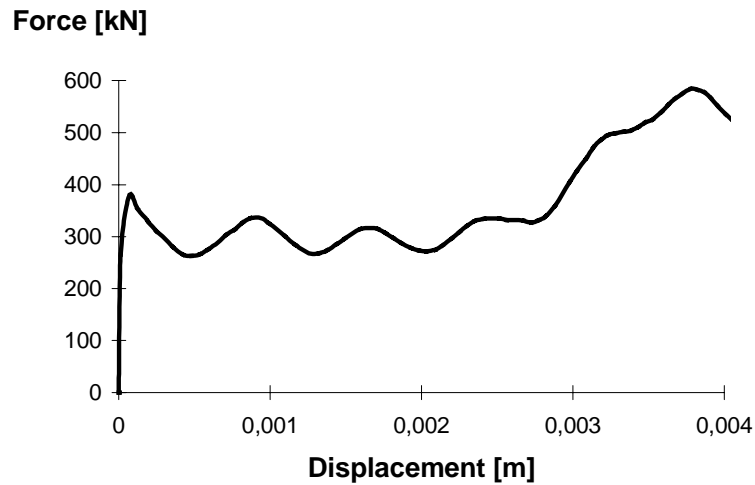


FIG.15. Force versus displacement for concrete 50 MPa, impactor mass = 78.3 kg, initial velocity of impactor $v_0= 5.3$ m/s

The change of impactor velocity is shown in the following Figures (Figs. 15, 16. and 17). This value was determined due to velocity of the contact nodes of the impactor versus time. Negative value of the characteristic describe the change of direction of the impactor movement. These characteristics were computed as a change of displacement of impactor nodes in time. The initial velocity confirms assumed values. The short time of constant part of the characteristic is the time necessary to close up the gap between the specimen and the impactor.

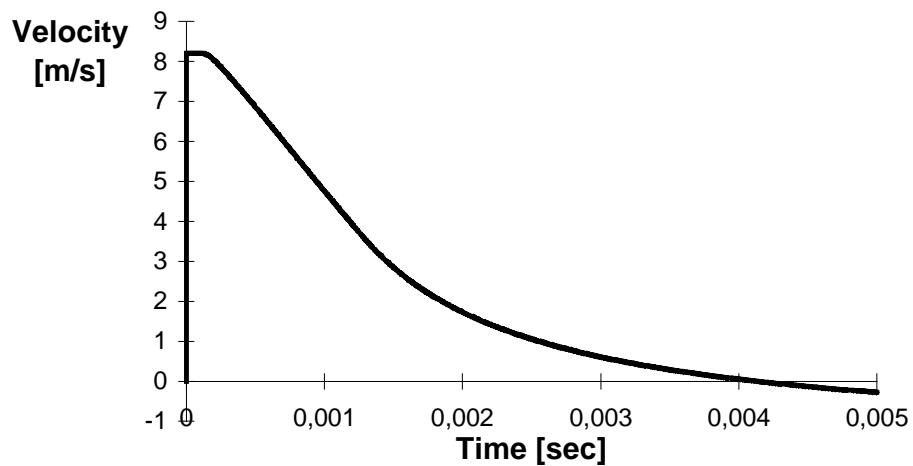


FIG. 16. Velocity of the impactor for concrete 30 MPa, impactor mass = 31.6 kg, initial velocity of impactor $v_0= 8.2$ m/s

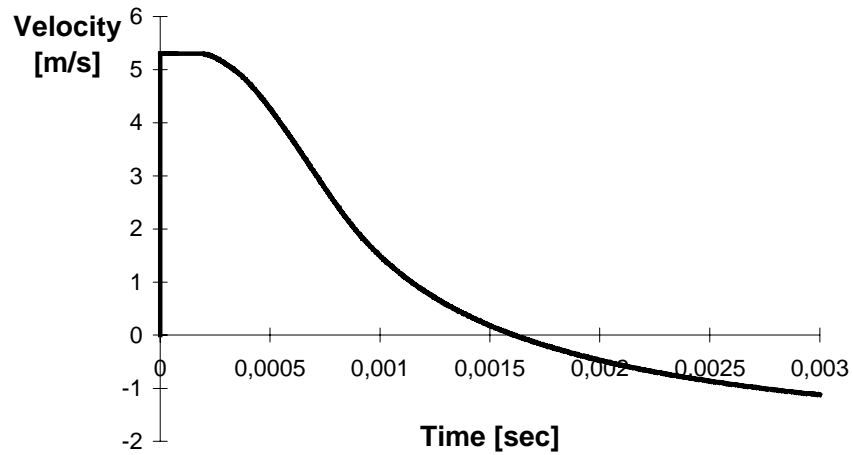


FIG. 17. Velocity of the impactor for concrete 50 MPa, impactor mass = 31.6 kg, initial velocity of impactor $v_0 = 5.3$ m/s

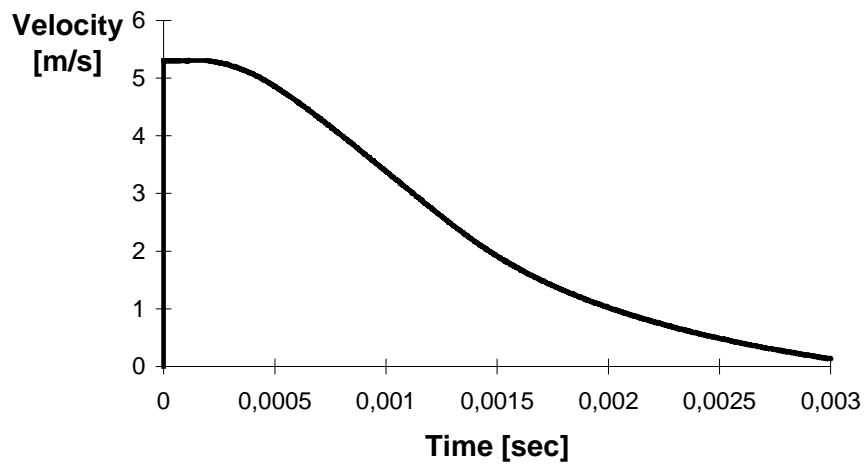


FIG. 18. Velocity of the impactor for concrete 50 MPa, impactor mass = 78.3 kg, initial velocity of impactor $v_0 = 5.3$ m/s

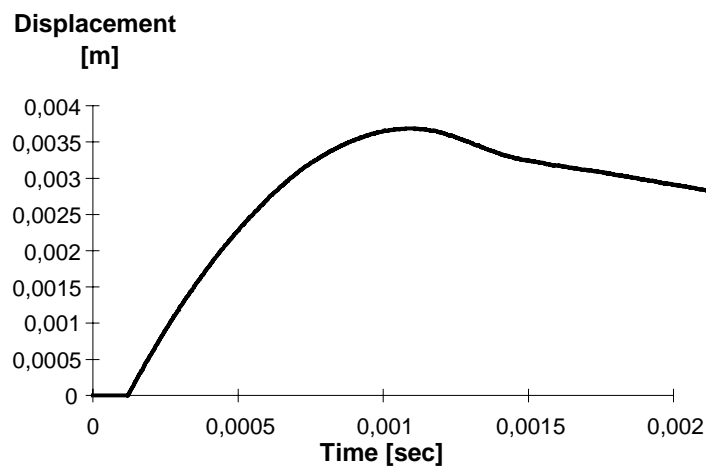


FIG. 19. Specimen displacement for concrete 30 MPa, impactor mass = 31.6 kg, initial velocity of impactor $v_0 = 8.2$ m/s

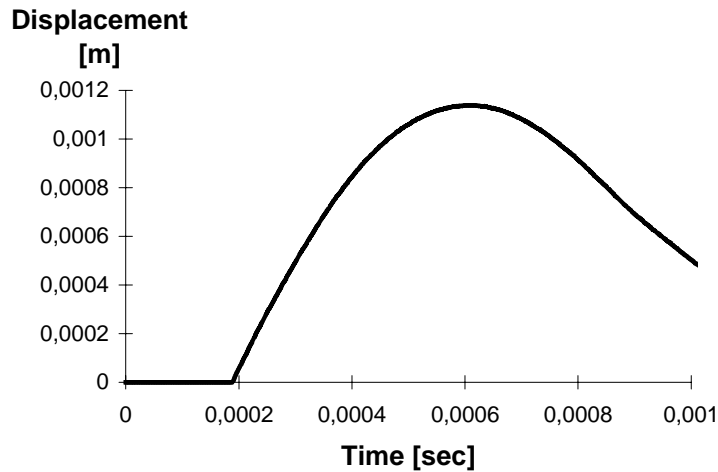


FIG. 20. Specimen displacement for concrete 50 MPa, impactor mass = 31.6 kg, initial velocity of impactor $v_0 = 5.3$ m/s

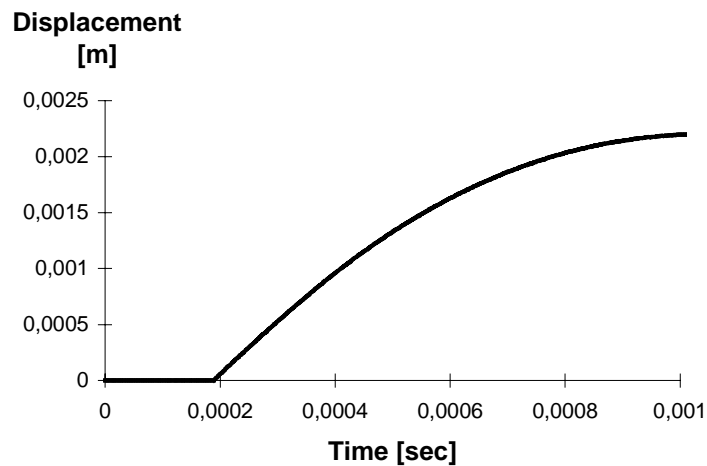


FIG. 21. Specimen displacement for concrete 50 MPa, impactor mass = 78.3 kg, initial velocity of impactor $v_0 = 5.3$ m/s

Figures 19, 20, and 21 show the deformation of the specimen, described as an average displacement of the contact nodes. In these plots the maximum shows the moment of mass reflection from the specimen. One can observe that only for relatively large mass the process of deformation does not exhibit the reflection.

Static numerical tests show good accuracy with experiments but the differences are still noticed, Figs. 22 and 23. The stresses were obtained as a reaction force at fixed end of the specimen converted to its cross section. The strain was computed as an average displacement of nodes on the loaded edge converted to specimen length. The differences are caused by discrete and surface-like experimental test. The strain gauges in experiments were placed at the surface of the specimen and values were taken in discrete way, while in numerical test the average value in cross section was consider in continuous way. In spite of these differences, the maximum values of stresses are similar in both cases. Numerical static tests consider

constitutive concrete models without any failure criterion this may also influence an important factor causing differences.

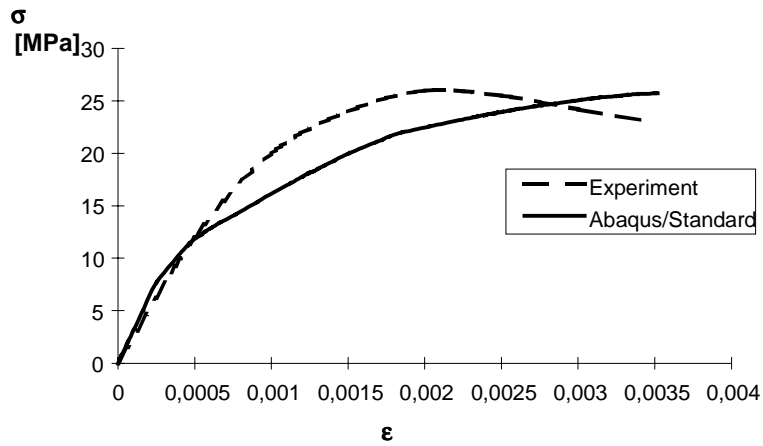


FIG. 22. Characteristics $\sigma - \varepsilon$ for concrete 30 MPa, static test.

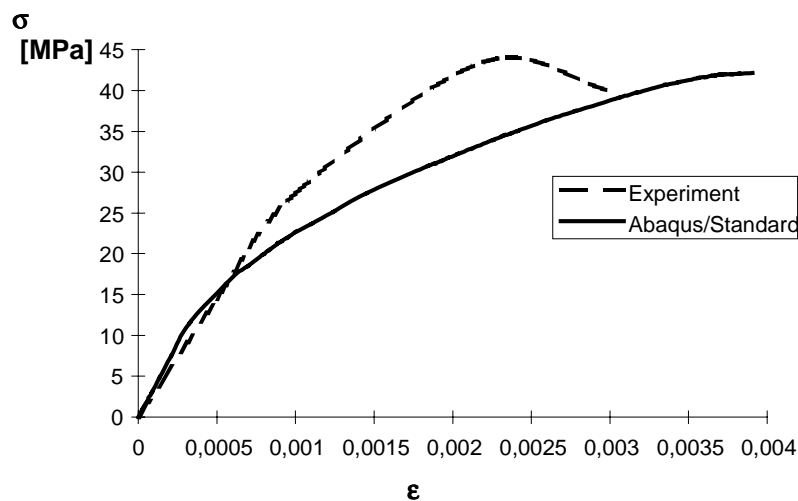


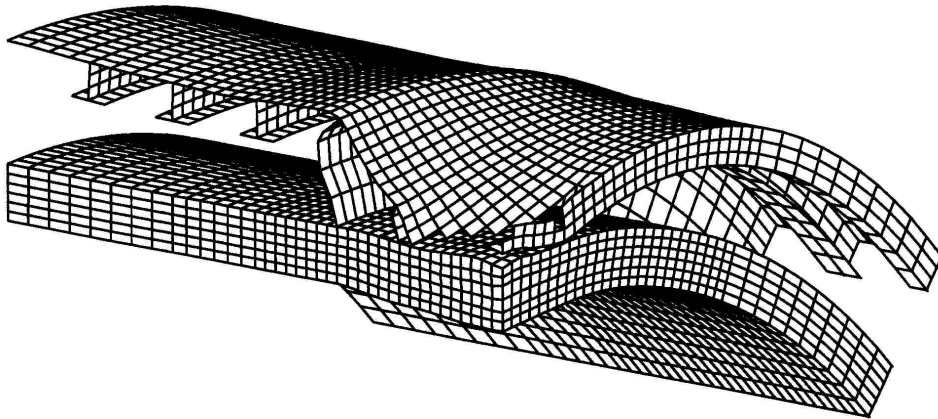
FIG. 23. Characteristics $\sigma - \varepsilon$ for concrete 50 MPa, static test.

6. Example of application

The new constitutive material model we applied to the analysis of complex engineering structure. The structure is an underwater tunnel loaded by explosion of 40 kg of spherical charge of trinitrotoluene (described in details in [9]). The structure consists of concrete and steel parts (shells). The distribution of pressure was obtained on the basis of semiempirical equations proposed by Henrych [10]. For the reasons of natural scale and type of loading, the structure could not be laboratory tested and its behaviour can be estimated only in numerical

way. In comparison, we considered two material models for concrete: Drucker-Prager model, available in ABAQUS code, and our rate dependent, elastic-plastic with tensile failure criteria elaborated in uniaxial laboratory tests and numerical simulations. The results of comparisons for those two models are in Figs. 24 and 25. The deformed meshes of structures are in Fig. 24. Fig. 25 shows equivalent plastic strains in concrete layer of sandwich, the main structural layer of the tunnel.

a)



b)

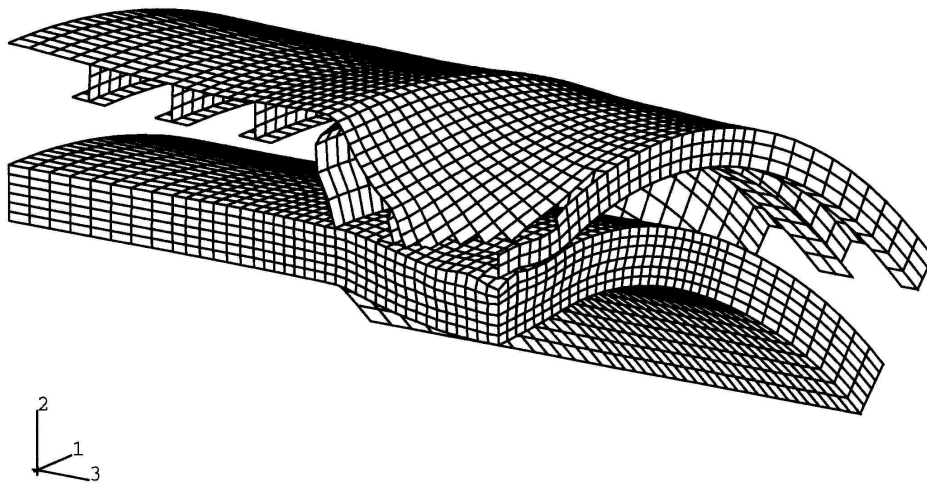


FIG. 24. Deformed meshes of underwater tunnel structure

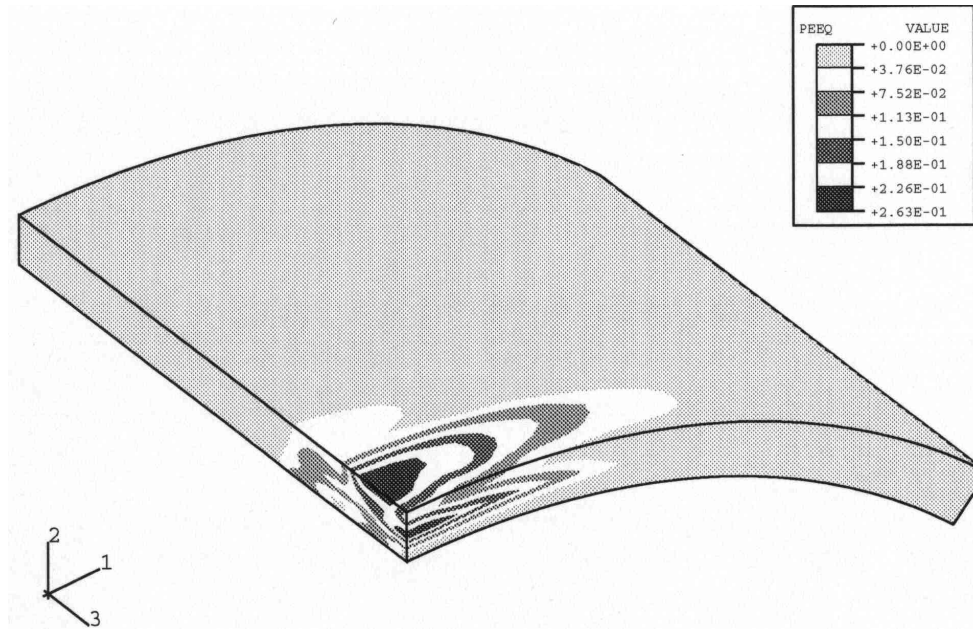
a) Drucker-Prager model for concrete

b) Rate dependent, elastic-plastic model with tensile failure criteria

For our new constitutive model of concrete, the structure reveals greater progress of concrete core deformation. It means, that in this case the area of destruction in concrete is larger then in case with constitutive model of Drucker-Prager. This observation is confirms

Fig. 25, which shows the contour plots of equivalent plastic strain in concrete layer of sandwich. However, the results in both cases confirm the validity of the idea of solving complex engineering problems only in numerical way, using the constitutive relations calibrated by simple laboratory tests.

a)



b)

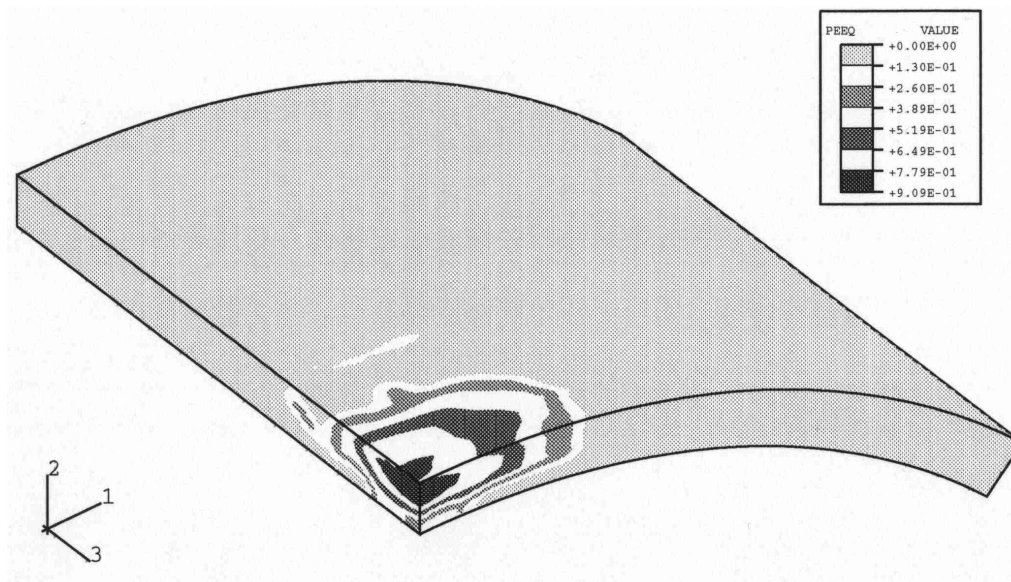


FIG. 25. Equivalent plastic strains in concrete layer of the tunnel

a) Drucker-Prager model for concrete

b) Rate dependent, elastic-plastic model with tensile failure criteria

7. Conclusions

Concrete is the one of the engineering materials, that subjected to high rates of deformation, usually associated with impacts, shows the increase of value of elastic modulus, compressive strength and values associated with them.

The differences in experimental and numerical results cause mainly by simplifications taken in assumptions of the experiment and the way of interpreting the results. In the lab test the wave character of phenomenon is expected and, in fact it was not noticed because of discrete type of obtained results. In numerical simulation, the wave character is strongly observed. The measured values vary, what is not taken into consideration in the lab tests. The second drawback of interpreting the experimental results is the local type of some counted values, which are considered as average. Numerical simulations approach the experimental values but it can be easily proved that these values taken in different place of specimen significantly differ because of wave character of the processes. In experiments, the values of strain rates were treated as constant and average in whole specimen. Numerical simulation shows, that they vary in time and have local character.

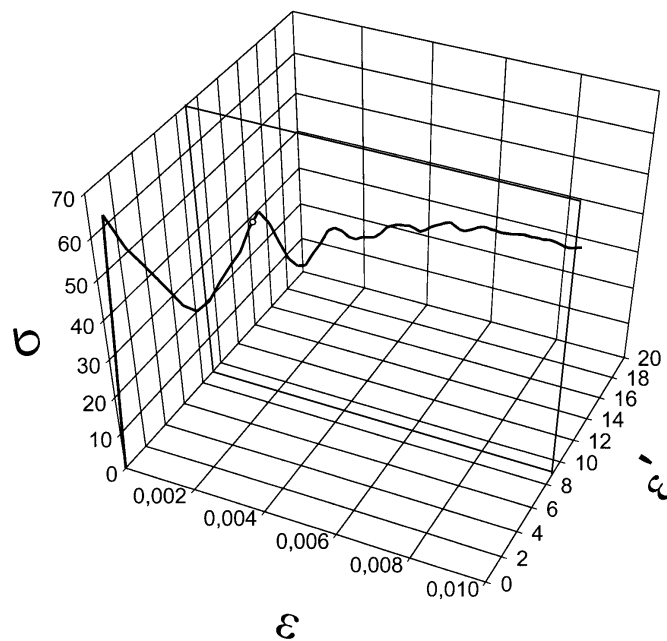


FIG. 26. Characteristic $\sigma - \varepsilon - \dot{\varepsilon}'$ for concrete 30 MPa, impactor mass = 31.6 kg, initial velocity of impactor $v_0 = 8.2$ m/s, estimated lab test $\dot{\varepsilon}' = 9$ [1/s].

Fig.26 shows the characteristic $\sigma - \varepsilon - \dot{\varepsilon}'$ for the first case considered in this paper (concrete 30 MPa, impactor mass = 31.6 kg, initial velocity of impactor $v_0 = 8.2$ m/s, estimated lab test $\dot{\varepsilon}' = 9$ [1/s]). The characteristics obtained for another strain rates create trajectories, from which one can spread out a surface. This surface bases on boundary solutions for used concrete constitutive model.

A plane for constant value of strain rate 9 [1/s] is added to show estimated in lab test strain rate and its intersection with non constant diagram of strain rate obtained in numerical simulation.

The comparison of these two tests (experimental and numerical) confirms how difficult is to carry out the reliable experimental test. However, this simple uniaxial test is reliable enough to claim that the aim of calibration of constitutive concrete model in impact load was achieved. The constitutive model calibrated in this way may be used to solve complex engineering problems.

Numerical simulation is more flexible, more comfortable, cheaper and requires less financial efforts than experimental tests. In many cases, also in this under consideration, the laboratory experiments are not possible and the engineering decision can be only supported by numerical simulation. This stresses the importance of proper constitutive modelling of the materials.

Laboratory tests should be strongly supported by numerical analysis to avoid mistakes in interpreting of some results. There is a need to carry out numerical analysis before laboratory tests are done. The details of specimen response or material behaviour are estimated and this significantly helps to design the laboratory tests.

References

- [1] ABAQUS 5.8 *Manuals*, Hibbit, Karlson & Sorensen Inc., 1999.
- [2] P. H. Bischoff and S. H. Perry, *Impact behavior of plain concrete loaded in Uniaxial compression*, Journal of Engineering Mechanics, pp 685-693, Vol. 121, No. 6, June, 1995.
- [3] K. Cichocki, R. Adamczyk, M. Ruchwa, *Material modelling for structures subjected to impulsive loading*, Computer Assisted Mechanics and Engineering Sciences, **6**: 231-244, 1999.
- [4] Z. Szcześniak, *Modelowanie zachowania dynamicznego konstrukcji podziemnych w warunkach działania powietrznej fali uderzeniowej*, WAT Warszawa 1999.
- [5] P. Soroushian, K.B. Choi, A. Alhamad, *Dynamic constitutive behaviour of concrete*. J. ACI, Vol. 83, No. 2, pp 251-259, March-April, 1986.
- [6] S. H. Perry, P. H. Bischoff, *Measurement of the compressive impact strength of concrete using a thin loadcell*. Mag. of Concrete Res., 42(151),75-81, 1990.
- [7] A. Glema, T. Łodygowski, P. Perzyna, *Interaction of deformation waves and localization phenomena in inelastic solids*, Computer Methods in Applied Mechanics and Engineering, 183 pp 123 - 140, 2000.
- [8] G. Bąk, A. Stolarski, *Analiza nieliniowa prętowych ustrojów żelbetowych obciążonych impulsowo*, PAN, Warszawa 1990.
- [9] K. Cichocki, R. Adamczyk, M. Ruchwa. *Effect of protective coating on underwater structure subjected to an explosion*. In: R. de Borst et al., eds., Proceedings of Euro-C International Conference “*Computational modelling of concrete structure*”, 623-631, Balkema, Badgastein, Austria, 1998.
- [10] J. Henrych, *The Dynamics of Explosions and Its Use*. Elsevier, Amsterdam, 1979.